AMERICAN SOCIETY FOR MICROBIOLOGY | Journal of Virology®

PATHOGENESIS AND IMMUNITY

Gammaherpesvirus Colonization of the Spleen Requires Lytic Replication in B Cells

Clara Lawler,[a] Marta Pires de Miranda,[b] Janet May,[c] Orry Wyer,[a] J. Pedro Simas,[b] Philip G. Stevenson[a,d]

[a]School of Chemistry and Molecular Biosciences, University of Queensland, Brisbane, Australia
[b]Instituto de Medicina Molecular, Universidade de Lisboa, Lisbon, Portugal
[c]Division of Virology, University of Cambridge, Cambridge, United Kingdom
[d]Royal Children's Hospital, Brisbane, Australia

ABSTRACT Gammaherpesviruses infect lymphocytes and cause lymphocytic cancers. Murid herpesvirus-4 (MuHV-4), Epstein-Barr virus, and Kaposi's sarcoma-associated herpesvirus all infect B cells. Latent infection can spread by B cell recirculation and proliferation, but whether this alone achieves systemic infection is unclear. To test the need of MuHV-4 for lytic infection in B cells, we flanked its essential ORF50 lytic transactivator with *loxP* sites and then infected mice expressing B cell-specific Cre (CD19-Cre). The floxed virus replicated normally in Cre$^-$ mice. In CD19-Cre mice, nasal and lymph node infections were maintained; but there was little splenomegaly, and splenic virus loads remained low. Cre-mediated removal of other essential lytic genes gave a similar phenotype. CD19-Cre spleen infection by intraperitoneal virus was also impaired. Therefore, MuHV-4 had to emerge lytically from B cells to colonize the spleen. An important role for B cell lytic infection in host colonization is consistent with the large CD8$^+$ T cell responses made to gammaherpesvirus lytic antigens during infectious mononucleosis and suggests that vaccine-induced immunity capable of suppressing B cell lytic infection might reduce long-term virus loads.

IMPORTANCE Gammaherpesviruses cause B cell cancers. Most models of host colonization derive from cell cultures with continuous, virus-driven B cell proliferation. However, vaccines based on these models have worked poorly. To test whether proliferating B cells suffice for host colonization, we inactivated the capacity of MuHV-4, a gammaherpesvirus of mice, to reemerge from B cells. The modified virus was able to colonize a first wave of B cells in lymph nodes but spread poorly to B cells in secondary sites such as the spleen. Consequently, viral loads remained low. These results were consistent with virus-driven B cell proliferation exploiting normal host pathways and thus having to transfer lytically to new B cells for new proliferation. We conclude that viral lytic infection is a potential target to reduce B cell proliferation.

KEYWORDS B cell, Cre/*lox*, gammaherpesvirus, lytic infection, pathogenesis

Gammaherpesviruses infect lymphocytes, drive their proliferation, and predispose them to transformation. Human gammaherpesviruses, for example, Epstein-Barr virus (EBV) and Kaposi's sarcoma-associated herpesvirus (KSHV), persist in B cells, as does murine herpesvirus-4 (MuHV-4) (1), a murid gammaherpesvirus (2, 3). *In vitro* EBV drives autonomous B cell proliferation. However, *in vivo* EBV-infected B cells show evidence of passage through germinal centers (GC) (4), sites of T cell-dependent B cell proliferation and transition to a resting memory state (5). MuHV-4 colonizes GC B cells (6–8), and both EBV (9) and MuHV-4 (6, 7, 10) persist in memory-type B cells. Thus, GC exploitation seems to be a common gammaherpesvirus theme. MuHV-4-infected B cell proliferation depends on CD4$^+$ T cells (11), CD40 (12), BAFF receptor (13), and B cell

Received 17 December 2017 **Accepted** 9 January 2018

Accepted manuscript posted online 17 January 2018

Citation Lawler C, de Miranda MP, May J, Wyer O, Simas JP, Stevenson PG. 2018. Gammaherpesvirus colonization of the spleen requires lytic replication in B cells. J Virol 92:e02199-17. https://doi.org/10.1128/JVI.02199-17.

Editor Rozanne M. Sandri-Goldin, University of California, Irvine

Address correspondence to Philip G. Stevenson, p.stevenson@uq.edu.au.

major histocompatibility complex (MHC) class II expression (14), indicating close parallels with normal, antigen-driven proliferation. EBV host colonization also parallels normal B cell physiology (15).

At steady state, most EBV-infected B cells express few viral antigens (9). Therefore, to vaccinate against infection, it may be necessary to target earlier events. In EBV and KSHV, these precede clinical presentation and remain ill defined. For example, host entry routes are unknown. Contact histories and acute tonsillitis led to a hypothesis of oral acquisition for infectious mononucleosis (IM) (16). However, IM occurs at least a month after EBV acquisition (17, 18) and matches peak host exit rather than entry. Because infection is systemic, entry and exit need not occur at the same site.

In vitro, cell-free EBV can infect naive B cells, but all gammaherpesviruses also infect non-B cells. If these are the primary targets, infection could reach B cells via antibody-shielding cell-cell contacts. For EBV and MuHV-4, non-B cell infection involves antigenically distinct receptor binding events (19–21), and vaccination to block EBV binding to B cells does not reduce *in vivo* infection rates (22). MuHV-4 enters new hosts nasally, not orally (23), and first infects olfactory epithelial cells (24). Herpes simplex virus 1 (25) and murine cytomegalovirus (26) do so, too, implying that olfactory entry has been conserved over hundreds of millions of years of herpesvirus evolution. MuHV-4 spreads from the olfactory epithelium via infected dendritic cells (DC) and first infects B cells in the draining superficial cervical lymph nodes (SCLN) (27). Infection increases in the SCLN and then spreads to the spleen.

When mice lack B cells, SCLN infection remains modest, and splenic viral loads are severely reduced (28, 29). Thus, MuHV-4 requires B cell infection for normal systemic infection. For EBV, B cell infection is proposed to be sufficient for the whole viral life cycle (15). This would limit the opportunities for vaccine-induced immune control. However, MuHV-4 shows additional complexity. When given intraperitoneally (i.p.), it directly infects splenic marginal zone (MZ) macrophages and then spreads sequentially to MZ B cells, follicular dendritic cells, and follicular B cells before colonizing splenic GC (30), where there is B cell proliferation (8, 31). Intranasal (i.n.) MuHV-4 also reaches MZ macrophages, and the presence of lytically infected plasma cells in SCLN (30) suggests that spread to the spleen involves virion release into the efferent lymph. However, memory B cell recirculation from the SCLN could be another route. While GC entry by memory B cells has not been demonstrated *in vivo* (32, 33), some *in vitro* characteristics of IgM^+ memory B cells suggest that they might undergo further differentiation in GC (34). To test the capacity of MuHV-4-infected B cells to colonize the spleen, we disabled viral lytic infection in B cells. Thus, infection would be established in SCLN B cells but then not spread to other cell types. Marked attenuation of splenic colonization argued that infected memory B cells poorly enter new GC and supported the idea that host colonization requires sequential lytic infections, making viral lytic antigens potentially important vaccine targets.

RESULTS

B cell infection tracked by viral fluorochrome switching. To track B cell infection, we gave mice with B cell-specific Cre expression (CD19-Cre) i.n. MuHV-4 that carries a fitness-neutral expression cassette (21), switched by Cre from red to green fluorescence (MHV-RG) (Fig. 1a). By fluorochrome typing recovered viruses, we could determine what proportion had passed through a Cre^+ cell. Many studies of MuHV-4 have inoculated it into the lungs of anesthetized mice. We used a more natural upper respiratory tract infection. Lytic infection here, which peaks at approximately day 7, is less extensive than that in the lungs, making the kinetics of host colonization more protracted: nasal infection reaches the spleen at day 11 to 14, with peak titers at day 21 to 25. At day 7, MHV-RG recovered from noses showed $<2\%$ switching, so here B cells were not a significant target (Fig. 1b). In contrast MHV-RG recovered from SCLN showed $>50\%$ switching. Therefore, B cells were first infected in the SCLN. Spleens contained insufficient virus to analyze switching at day 7, but at day 14 splenic virus was almost completely switched.

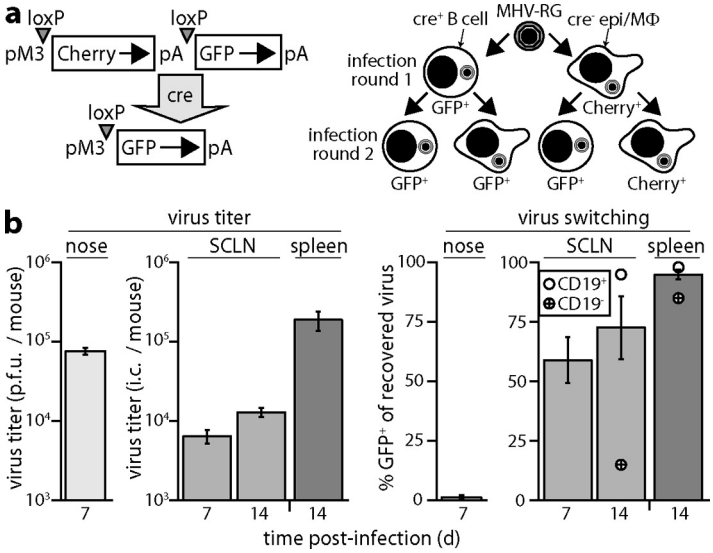

FIG 1 Cre/*lox* tracking of MuHV-4 spread from SCLN to spleens. (a) We used MuHV-4 with a color-switching cassette inserted between ORFs 57 and 58 (MHV-RG). An ectopic viral M3 (lytic) promoter drives expression of *loxP*-flanked Cherry (red). Cre removes Cherry plus its polyadenylation site. The M3 promoter then drives expression of GFP (green). During host colonization each virus follows a chain of infections, passing in CD19-Cre mice between Cre$^-$ epithelial/myeloid cells (epi/MΦ; shown as irregular shapes) and Cre$^+$ B cells (shown as round shapes). Passage through a Cre$^+$ cell switches MHV-RG irreversibly to GFP expression. (b) CD19-Cre mice were given MHV-RG i.n. to infect the upper respiratory tract. After 7 to 14 days, titers for GFP$^+$ and Cherry$^+$ virus loads were determined by plaque assay (PFU) or infectious center assay (i.c.) for noses, superficial cervical LN (SCLN), and spleens. Virus switching was calculated as follows: 100 × GFP$^+$ titer/(GFP$^+$ titer + Cherry$^+$ titer). Bars show means ± standard errors of the means of data for 6 mice. At day 14, SCLN and spleen cells, each pooled from 3 mice, were further sorted into CD19$^+$ B cells and CD19$^-$ non-B cells before the color switching of recovered viruses was determined (circles). d, day.

Sorting day 14 SCLN cells into B cells (CD19$^+$) and non-B cells (CD19$^-$) established that MHV-RG in B cells was almost entirely switched. Virus recovered from non-B cells, presumably myeloid cells (1), showed little switching, consistent with infection proceeding from olfactory epithelial cells (Cre$^-$) to myeloid cells (Cre$^-$) to B cells (Cre$^+$) (27). In spleens both B cell and non-B cell viruses were switched, consistent with infection spreading via SCLN B cells. However, because Cre-mediated recombination is a single-hit process, we could not tell whether the splenic B cells had been infected in the SCLN or in the spleen. Nor could we distinguish these possibilities in mice with myeloid cell-specific Cre expression as MuHV-4 reaches the SCLN via myeloid cells and so again is switched before reaching the spleen (21).

Conditional inactivation of MuHV-4 lytic infection. To define better how olfactory infection reaches splenic B cells, we generated a virus in which Cre/*lox* recombination inactivates lytic infection (Fig. 2). MuHV-4 initiates lytic infection via its ORF50 transactivator: ORF50$^-$ mutants do not replicate without complementation (35) and when inoculated i.n. do not reach the spleen (36). ORF50$^-$ MuHV-4 inoculated i.p. infects splenic MZ macrophages but not B cells (30). This reflects splenic anatomy (MZ macrophages filter the blood) and viral tropism (MuHV-4 must pass through myeloid cells to gain B cell tropism) (21). ORF50 has two exons that span ORF49 (Fig. 2a). ORF49 encodes a tegument protein that interacts with ORF50 to promote lytic infection (37). We inserted *loxP* sites between open reading frames (ORFs) 48 and 49 and between ORFs 50 and M7 (MHV-F50), using an altered spacer region to make these sites incompatible with the *loxP* sites flanking the viral bacterial artificial chromosome (BAC) cassette (38). Removal of ORF49 and ORF50 by virus passage through Cre$^+$ cells was confirmed by PCR amplification across this locus (Fig. 2b).

MHV-F50 was severely attenuated for replication in Cre$^+$ fibroblasts (Fig. 2c). Using a derivative that expresses green fluorescent protein (GFP) from an intergenic EF1α

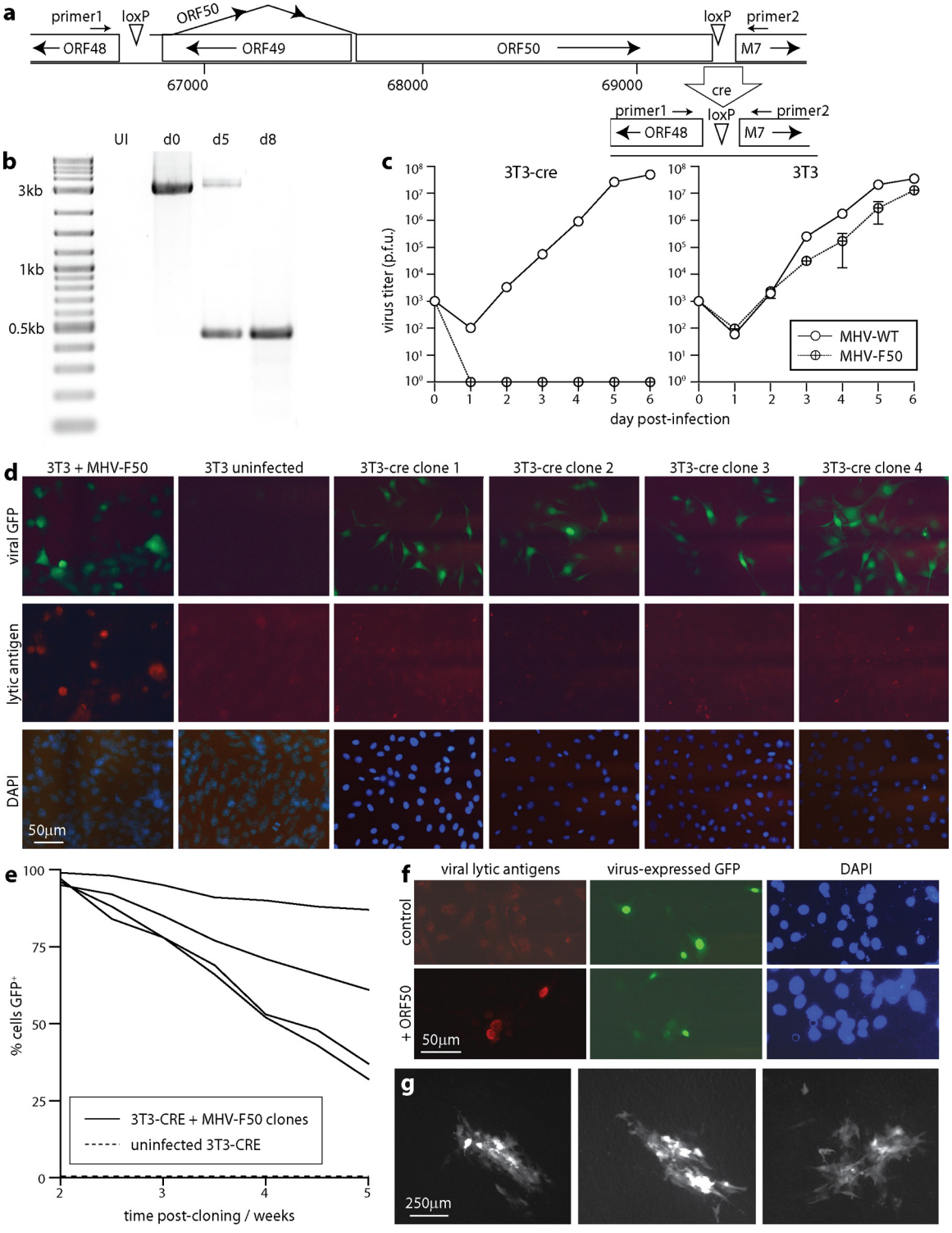

FIG 2 Cre-dependent inactivation of MuHV-4 lytic infection. (a) To conditionally inactivate MuHV-4 lytic infection, we inserted *loxP* sites between ORFs 48 and 49 and between ORFs 50 and M7 (MHV-F50). Thus, *loxP* recombination removed ORF49 and both exons of ORF50. (b) To visualize this recombination, we infected 3T3-Cre cells (0.1 PFU/cell); 0, 5, and 8 days later we extracted DNA from the cultures and performed PCR amplification across ORFs 49 and 50 as indicated in panel a. UI, uninfected. The 3-kb band corresponds to the native, unrecombined locus. The 0.5-kb band corresponds to the locus after recombination. (c) We compared wild-type (MHV-WT) and MHV-F50 growth in Cre$^+$ (3T3-Cre) and Cre$^-$ (3T3) fibroblasts. Cells were infected (0.01 PFU/cell, 2 h), exposed to pH 3 to inactivate nonendocytosed virions, washed in PBS, and cultured at 37°C. Virus titers in replicate cultures were determined by plaque assay daily thereafter. Each point shows means ± standard errors of the means of triplicate cultures. Time zero shows the virus input. (d) We infected 3T3-Cre cells with GFP$^+$ MHV-F50 and derived GFP$^+$ cell clones. These were then stained for MuHV-4 lytic antigens with a polyclonal rabbit serum. Four clones are shown at 5 weeks after cloning, in comparison with positive (infected 3T3 cell) and negative (uninfected 3T3 cell) controls. No

(Continued on next page)

promoter independently of lytic infection (39), we established GFP-positive (GFP^+) clones of virus-exposed Cre^+ fibroblasts that showed no lytic gene expression (Fig. 2d). These clones showed some loss of GFP expression with continued culture (Fig. 2e), as occurs also when MuHV-4 is kept latent by ORF50 transcriptional suppression (40). Nonetheless, lytic infection could be initiated by transduction with an ORF50-positive ($ORF50^+$) retrovirus (Fig. 2f), and the MHV-F50 recovered from cell supernatants could then be propagated in $ORF50^+$-complementing fibroblasts (Fig. 2g). It could not be propagated in noncomplementing fibroblasts. Therefore, MHV-F50 was inactivated for lytic replication by Cre but was retained in a viable, latent form that could be recovered by exogenous ORF50.

Early MHV-F50 infection in Cre^+ mice. We gave MHV-F50 i.n. to $CD19^{+/Cre}$ (CD19-Cre) mice and $CD19^{+/+}$ (wild type [WT]) littermate controls (Fig. 3). Typically, nasal infection peaks at day 7, SCLN infection peaks at day 11, and splenic infection peaks at day 20 to 30. At day 7 nasal virus titers were no different between WT and CD19-Cre mice (Fig. 3a), consistent with the lack of MHV-RG switching in this site (Fig. 1b). At day 11, MHV-F50 SCLN infection in CD19-Cre mice was not significantly less than that in WT MuHV-4 or MHV-F50 infection in WT mice (Fig. 3b). At the same time point MHV-F50 infection in CD19-Cre spleens was significantly reduced.

SCLN infection has both myeloid and B cell components. The myeloid component was expected to be normal. However, MHV-F50 B cell infection should have been impaired in CD19-Cre mice, so it was surprising to see no significant reduction in recovery of replication-competent virus. This indicated a lack of recombination as ORF50 loss completely prevents MuHV-4 lytic replication (35, 36), and PCR across the ORF50 locus, as illustrated in Fig. 2b, confirmed on multiple occasions that the replication-competent MHV-F50 recovered from CD19-Cre SCLN was not recombined. The most likely explanation was inefficient excision of MHV-F50 ORF49 by Cre. We used $CD19^{+/Cre}$ mice, which express less Cre than $CD19^{Cre/Cre}$ mice (41) as $CD19^{Cre/Cre}$ mice are CD19 deficient (42); in addition, many infected B cells differentiate to plasma cells (43), which downregulate CD19 (44). Thus, Cre expression was possibly low in some infected B cells, and MHV-F50 attenuation must be considered only a minimum estimate of the need for MuHV-4 to pass through B cells.

We assayed day 11 MHV-F50 infection also in CD11c-Cre (Fig. 3c) and LysM-Cre mice (Fig. 3d). In a comparison of CD11c-Cre mice with littermate controls, MHV-F50 showed a Cre-dependent defect in SCLN infection, consistent with MuHV-4 reaching the SCLN via $CD11c^+$ DC (27). However, there was no significant defect in spleen infection. DC infection is not uniformly lytic (45), so early (day 11) splenic infection may derive from DC that rapidly produce new virus, while the infection still in SCLN at day 11 presumably includes DC with slower virus production and thus longer exposure to Cre.

The normal SCLN infection and reduced splenic infection of LysM-Cre mice by MHV-F50 was consistent with splenic infection proceeding via $LysM^+$ MZ macrophages (30).

Steady-state MHV-F50 infection in CD19-Cre mice. We then tracked MHV-F50 in CD19-Cre mice up to day 35 (steady state) and compared the results with those of WT mice given the same virus (Fig. 4). Colonization of CD19-Cre SCLN showed a significant defect at all time points after day 7. CD19-Cre spleens also showed significant infection

FIG 2 Legend (Continued)
lytic antigen expression was evident in the cloned GFP^+ Cre^+ cells. (e) GFP expression of cell clones as illustrated in panel d was determined by flow cytometry during *in vitro* passage. GFP expression declined with time in all clones. Nonetheless, it was maintained in a substantial proportion of cells, implying that recombined viral genomes were maintained. (f) After passage for 7 weeks, infected 3T3-Cre cell clones were transduced or not (control) with $ORF50^+$ retrovirus. Five days later they were stained for viral lytic antigens as described for panel d. A representative example is shown. Not all lytic antigen-positive cells were GFP^+, suggesting that at least some of the loss of viral GFP expression in the experiment shown in panel e was due to cassette silencing. No untransduced cells were lytic antigen positive. (g) Supernatants of the retrovirus-transduced cultures in shown in panel f were used to infect NIH 3T3-ORF50 cells. Infection was then identified by viral GFP expression. Three representative images are shown of plaques (clusters of >50 infected cells) developing 3 days after addition of cell supernatants. This rescue by exogenous ORF50 established that the recombined viral genomes maintained in NIH 3T3-Cre cells were otherwise viable.

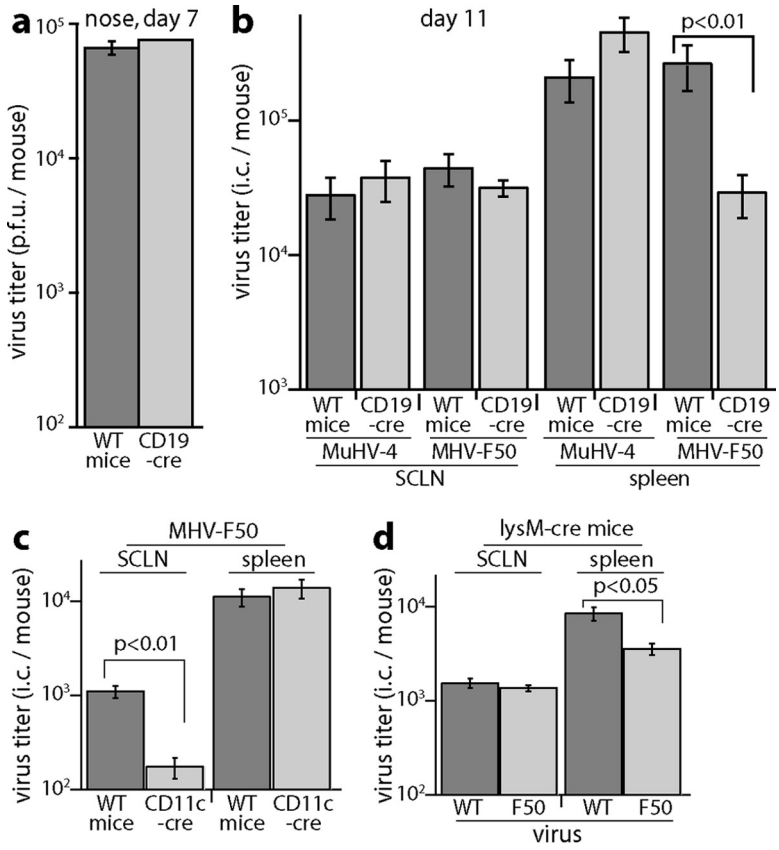

FIG 3 Early lymphoid infection by MHV-F50. (a) We infected CD19-Cre mice or Cre$^-$ littermate controls (WT) i.n. with MHV-F50. Plaque assays showed no significant difference in nose titers 7 days later. Bars show means ± standard errors of the means of titers of 6 mice per group. (b) WT or CD19-Cre mice were given i.n. MHV-F50 or WT MuHV-4. Eleven days later virus titers in SCLN and spleens were determined by infectious center (i.c.) assay. There was no difference in SCLN titers, but MHV-F50 titers were significantly reduced in CD19-Cre spleens. Bars show means ± standard errors of the means of titers of 6 mice per group. (c) CD11c-Cre or WT mice were given i.n. MHV-F50. Eleven days later virus loads in SCLN and spleens were determined by infectious center assay. F50 titers were significantly reduced in SCLN but not in spleens. Bars show means ± standard errors of the means of titers of 6 mice per group. (d) LysM-Cre mice were given i.n. MHV-F50 (F50) or WT MuHV-4 (WT). Eleven days later virus loads in SCLN and spleens were determined by i.c. assay. MHV-F50 titers were equivalent to those of the WT in SCLN and significantly reduced in spleens. Bars show means ± standard errors of the means of titers of 6 mice per group.

defects at days 14, 23, and 35, with a significantly greater defect after day 14 (Fig. 4a). Thus, Cre-dependent MHV-F50 attenuation increased with time. The completeness of viral genome recombination in individual B cells may increase with time. However, latent viral genomes undergo chromatinization (46), which is associated with reduced accessibility to Cre (47). Viral genomes are not chromatinized when they enter cells, so this may be when they are most likely to be recombined by Cre. More recombination with time would then be most likely to reflect additional passages through B cells.

Splenomegaly, which was most obvious in WT mice at day 23, was greatly reduced in CD19-Cre mice (Fig. 4b). WT and CD19-Cre mice showed no obvious difference in the degree of SCLN enlargement. MHV-F50 DNA loads were similar in WT and CD19-Cre mice at day 14 and reduced in CD19-Cre mice thereafter, with spleens showing the most marked differences (Fig. 4c). Sorting CD19$^+$ cells confirmed that MHV-F50 genome loads were reduced in CD19-Cre B cells (Fig. 4d).

We visualized splenic infection by *in situ* hybridization for viral tRNA/miRNAs 1 to 4 (48) (Fig. 4e). In WT spleens, MHV-F50 showed positive signals in scattered cells at day 14 and strong GC signals at day 23. CD19-Cre spleens lacked detectable signals. Therefore, by multiple measures MHV-F50 showed a marked splenic infection defect in CD19-Cre mice.

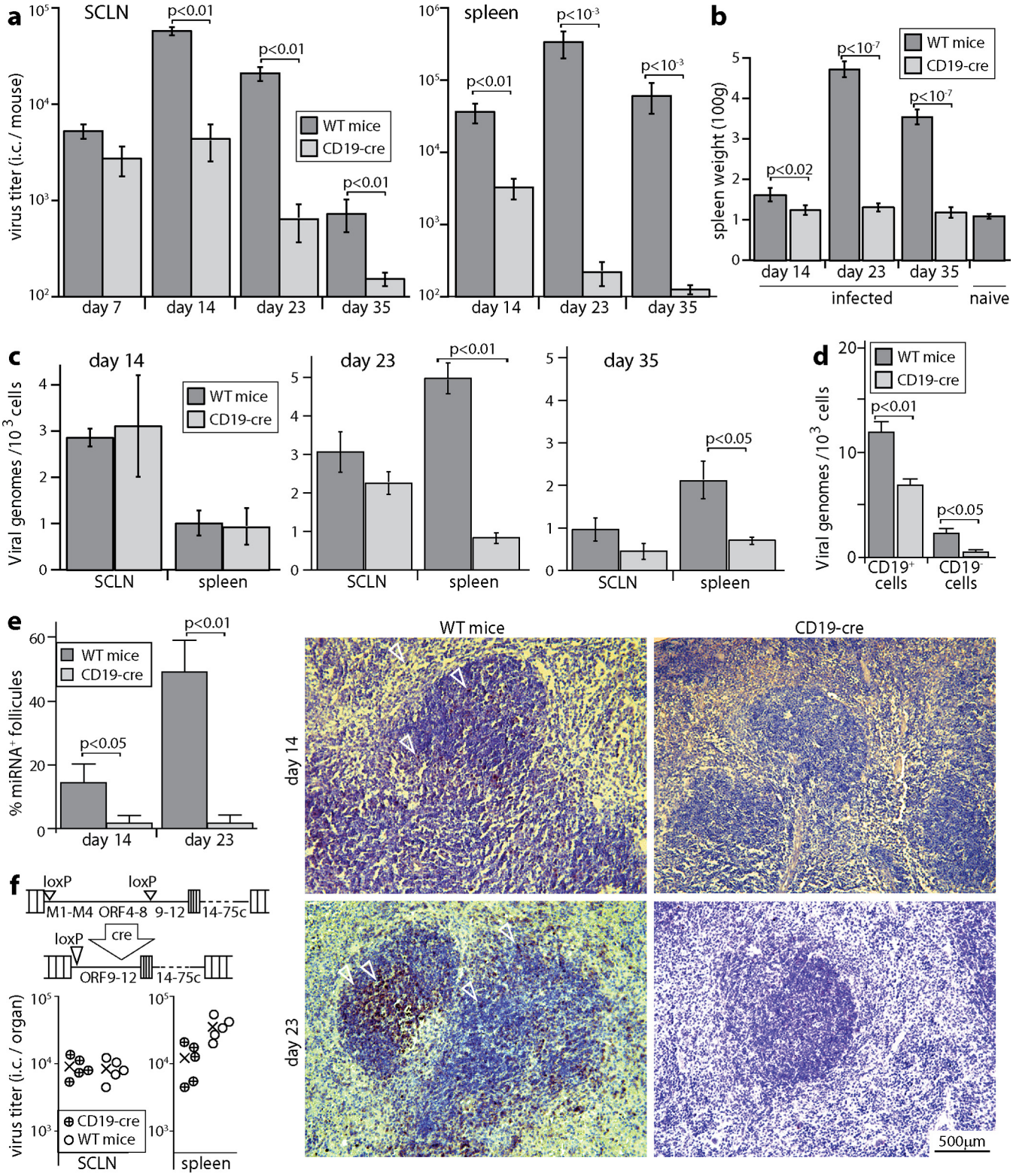

FIG 4 Longer-term lymphoid infection by MHV-F50. (a) CD19-Cre mice or Cre$^-$ littermate controls (WT) were given i.n. MHV-F50. Infectious center assays recovered significantly less virus from CD19-Cre SCLN and spleens from day 14 onwards. (b) For mice from the experiment shown in panel a, spleen weights were significantly lower in CD19-Cre mice. Bars show means ± standard errors of the means of 6 mice per group. (c) The samples from the experiment shown in panel a were assayed for viral genome load by quantitative PCR of purified DNA. CD19-Cre spleens yielded significantly fewer viral genomes per cell at day 23 and day 35. (d) CD19-Cre and WT mice were infected with MHV-F50 as described for panel a, and at day 23 spleen cells were sorted into CD19$^+$ and CD19$^-$ subsets. Viral genome loads were assayed for each by quantitative PCR and were significantly reduced in CD19-Cre mice. (e) CD19-Cre and WT mice were infected as described for panel a. At day 14 and day 23, spleens were fixed, and sections were probed for expression of viral tRNAs/miRNAs 1 to 4 by *in situ* hybridization. Positive signals are shown in black. Sections were counterstained with hematoxylin (purple). The graph shows counts (means ± standard errors

(Continued on next page)

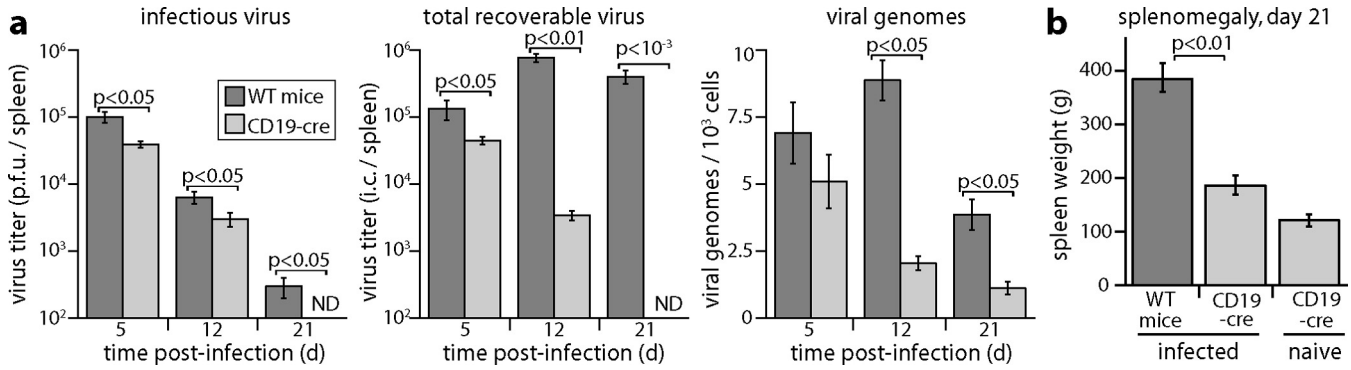

FIG 5 Infection by i.p. inoculation with MHV-F50. (a) We gave CD19-Cre or WT mice MHV-F50 i.p. (10^5 PFU) and 5, 12, and 21 days later assayed preformed infectious virus by plaque assay, total recoverable virus (preformed plus reactivation-competent latent virus) by infectious center assay, and viral genome loads by quantitative PCR. Bars show titers (means ± standard errors of the means) of 6 mice per group. ND, not detected. (b) Spleen weights of the day 21 mice from the experiment shown in panel a showed significantly less MHV-F50-driven splenomegaly in CD19-Cre mice than in WT controls. Bars show titers (means ± standard errors of the means) of 6 mice per group.

MuHV-4 inactivation by left-end genome excision. We also tested host colonization by MuHV-4 with *loxP* sites flanking the left-hand 19 kb of its genome (MHV-F8/9) (Fig. 4f). BAC-derived MuHV-4 retains a *loxP* site at the left end of its unique genome sequence after BAC cassette excision (38). MHV-F8/9 has a compatible *loxP* site inserted between ORF8 and ORF9 (27). The flanked sequence includes ORFs 6 to 8, which are essential for lytic infection, so again *loxP* recombination terminated viral spread to new cells. Recombined MHV-F8/9 may also be impaired in latent genome survival as it loses M1 to M4, viral tRNA/miRNAs 1 to 8, and a likely transcription start site for ORF73 (49). This was not explored in detail as we wanted mainly to confirm the Cre-dependent attenuation of MHV-F50. At day 23 of i.n. infection, MHV-F8/9 showed no significant defect in SCLN infection of CD19-Cre mice but a significant defect in spleen infection. The MHV-F8/9 infection defect was less marked than that of MHV-F50, perhaps because the 19-kb-spaced *loxP* sites of MHV-8/9 were less efficiently recombined than the 3-kb-spaced *loxP* sites of MHV-F50. Nonetheless, MHV-F8/9 infection was qualitatively similar in being reduced mainly in the spleen.

Splenic infection by i.p. MHV-F50. B cells infected in the SCLN presumably recirculate through the splenic MZ, but they were unable to colonize splenic GC. To test whether MHV-F50 could colonize CD19-Cre spleens if SCLN B cells were bypassed, we gave it i.p. (Fig. 5). MuHV-4 inoculated i.p. enters the spleen via MZ macrophages and then passes sequentially to MZ B cells, follicular DC, and follicular B cells (30). Thus, there is still a need to pass through B cells to reach GC. In MZ macrophages, i.p. MuHV-4 is mainly lytic; in follicular B cells it is mainly latent (29).

After i.p. inoculation, day 5 lytic infection showed only a small (<10-fold) difference in titers between the spleens of CD19-Cre mice and those of WT mice (Fig. 5a). This result was consistent with MHV-F50 replicating normally in Cre^- MZ macrophages. At day 5 of i.p. infection, most splenic infection is lytic, so the difference in total recoverable virus (lytic plus latent) was also small. At day 12 and day 21, when infection had progressed to B cells (Cre^+) and was mostly latent, CD19-Cre mice showed a larger (>100-fold) reduction in total recoverable virus. Viral genome loads also showed a larger defect at day 12 than at day 5 (Fig. 5a), so this was not just a difference in reactivation; and CD19-Cre mice had significantly less infection-driven splenomegaly (Fig. 5b). These results were consistent with MHV-F50 passing poorly through Cre^+ MZ

FIG 4 Legend (Continued)
of the means) of tRNA/miRNA-positive follicles for at least three sections from each of 3 mice per group. Representative images are shown. Arrows indicate example positive cells. (f) We tested also MuHV-4 in which *loxP* sites flank the unique left end of the viral genome from its start up to ORF9 (MHV-F8/9). This allows Cre to remove the essential ORFs 6 to 8. We gave WT and CD19-Cre mice i.n. MHV-F8/9 and determined virus titers by infectious center assay at day 23. MHV-F8/9 showed somewhat less Cre-dependent attenuation than MHV-F50 but a similar pattern of reduced splenic rather than SCLN colonization.

B cells and thus poorly colonizing follicular B cells to generate GC. B cells infected in the splenic MZ evidently failed to participate efficiently in GC formation.

DISCUSSION

The capacity of B cells for proliferation, longevity, and systemic migration makes them a prime target for viral infections. GC exploitation allows gammaherpesviruses to increase massively infected B cell numbers. This drives acute lymphadenopathy and splenomegaly. The naive B cells that enter GC are segregated from mucosal surfaces: they recirculate through lymph nodes (LN) and meet antigens only after they have been captured by myeloid cells. MuHV-4 copes with this inaccessibility by infecting myeloid cells. The compartmentalization of *in vivo* B cell populations further mandates viral lytic replication for systemic spread as latently infected LN B cells poorly colonized splenic GC.

Because B cells enter GC as naive cells and exit as memory cells, they cannot freely cycle through multiple GC reactions. This applied also to MuHV-4-infected B cells. We conclude that to exploit GC serially, gammaherpesviruses must transfer lytically from memory back to new, naive B cells. An important role for lytic infection in B cell colonization is consistent with the large acute $CD8^+$ T cell responses made to lytic antigens during MuHV-4-induced (50) and EBV-induced IM (51). It explains why Blimp-1 deficiency, which impairs plasma cell differentiation and hence MuHV-4 reactivation, impairs latency establishment (52). It may explain also why MuHV-4 lacking M2, which promotes reactivation (53), poorly reaches splenic GC (54).

Upon MuHV-4 rechallenge of immune mice, splenomegaly does not recur. EBV-driven IM also seems to occur just once. Thus, antiviral immunity limits GC colonization. Analysis of EBV control has focused on recognizing viral latency gene products that drive B cell proliferation *in vitro*. However, vaccination to prime such responses did not reduce viral loads (55). T cell transfers reduce EBV-driven lymphoproliferation in immunocompromised patients. However, they include $CD4^+$ and $CD8^+$ T cells with multiple antigen specificities, and lytic antigen-specific $CD4^+$ T cells may be an important component (56). $CD8^+$ T cell recognition of the M2 latency gene limits long-term MuHV-4 loads (57), but priming this response gave no further reduction (58). Protection against WT MuHV-4 by infection with latency-deficient mutants (59–61) supports the idea that immunity to lytic antigens can reduce latent viral loads. A need for lytic infection to colonize GC would explain why. MuHV-4 reaches naive B cells via lytically infected myeloid cells. $CD4^+$ T cells control myeloid infection; $CD8^+$ T cells control epithelial infection well but control myeloid infection poorly due to viral evasion (62). This may explain why priming lytic antigen-specific $CD8^+$ T cells failed to reduce latent viral latent loads (63). Priming lytic antigen-specific $CD4^+$ T cells might be more effective.

Gammaherpesvirus-driven splenomegaly is associated with generalized lymphadenopathy and with infection spreading to submucosal sites such as nasal-associated lymphoid tissue (21). Thus, we envisage that systemic lymphoid colonization involves multiple rounds of GC exploitation, with both LN-derived and spleen-derived memory B cells seeding new naive B cell infections. Latent infection is then maintained despite ongoing reactivation for transmission. Antigen-specific B cell memory does not suffer from the same attrition, so homeostatic memory B cell proliferation alone seems unlikely to maintain latent viral loads. Rather, new B cell infection and GC exploitation must continue long-term. Consistent with this idea, MHV-F50 attenuation increased with time. This would imply that the immune control of lymphoproliferation is incomplete, much as the control of virus shedding is incomplete. Nonetheless latency-deficient vaccines show that long-term lymphoid colonization can be kept to a very low level.

A need for ongoing lytic infection to establish and maintain viral latent loads also opens up the possibility of reducing latency with anti-lytic cycle drugs. Ganciclovir reduces the risk of Kaposi's sarcoma (KS) in AIDS (64). Inhibiting EBV lytic infection with acyclovir has no obvious impact on IM (65). However, this report was based on a short

course of treatment given when GC colonization was already at its height; when given long-term, acyclovir reduces EBV latent loads (66). Other drugs more potently inhibit EBV lytic infection (67). Their efficacy will depend ultimately on the lytic turnover rate of gammaherpesviruses, which is yet to be determined. The present data establish that latency alone in B cells does not suffice for host colonization, so lytic-based therapies have the potential to limit latent infection.

MATERIALS AND METHODS

Mice. C57BL/6J, CD19-Cre (42), CD11c-Cre (68), and LysM-Cre mice (69) were kept at University of Queensland animal units. The *cre* alleles were maintained by heterozygote × nontransgenic breeding. Mice were given MuHV-4 (10^5 PFU) when 6 to 8 weeks old, either i.n. in 5 μl without anesthesia to inoculate the upper respiratory tract (70) or i.p. Animal experiments were approved by the University of Queensland Animal Ethics Committees in accordance with Australian National Health and Medical Research Council (NHMRC) guidelines. Statistical comparison was by heteroscedastic Student's two-tailed unpaired *t* test unless otherwise stated.

Cells and viruses. Baby hamster kidney (BHK-21) fibroblasts (American Type Culture Collection CCL-10), NIH 3T3 (CRL-1658), NIH 3T3-Cre (71), and NIH 3T3-ORF50 (23) cells were grown in Dulbecco's modified Eagle's medium with 2 mM glutamine, 100 IU/ml penicillin, 100 μg/ml streptomycin, and 10% fetal calf serum (complete medium). MHV-GFP (39) expresses GFP from an EF1α promoter inserted between the 3′ ends of ORFs 57 and 58. MHV-RG (30) has in the same site an ectopic viral M3 (lytic) promoter driving the transcription of *loxP*-flanked mCherry plus a stop cassette upstream of GFP. Thus, it forms mCherry-positive (mCherry$^+$) plaques (red) until recombined by Cre, when it switches to forming GFP$^+$ plaques (green). MHV-F8/9 (27) has a *loxP* site inserted at genomic coordinate 19055, between ORFs 8 (glycoprotein B) and 9 (DNA polymerase). This can pair with a *loxP* site which remains at the left end of the BAC-cloned viral genome between the terminal repeats and viral tRNA1 after the BAC cassette is excised (38). Thus, *loxP* recombination by Cre deletes a 19-kb genomic segment that includes viral tRNAs 1 to 8 and ORFs M1 to M4, 4, 6, 7, and 8. ORFs 6, 7, and 8 are essential to make infectious virions (72). To prevent lytic cycle initiation, we inserted *loxP* sites around a 2.5-kb genomic segment incorporating ORF50 (MHV-F50). Its transcription initiates between ORFs 48 and 49 (73). We amplified by PCR genomic coordinates 65100 to 66601, adding an SphI site at position 65100 and a *loxP* site at 66601. We then amplified genomic coordinates 66602 to 68097, adding a *loxP* site at position 66602 and an SalI site at 68097, just downstream of a genomic BstBI site (68088). The downstream primer also incorporated a silent mutation in ORF50 at position 68084 to inhibit subsequent recombination of this segment by RecA and thus promote the insertion of both *loxP* sites rather than just one. The 34-bp *loxP* site comprises 13 bp of complementary recognition regions, which are invariant, and an intervening 8-bp spacer region, which can vary except for the central two bases. Cre recombines *loxP* sites only when their spacer regions match. The *loxP* sites introduced around ORF50 had an altered spacer region (GGATACTT), making them incompatible with those surrounding the viral BAC cassette (GCATACAT). The PCR products were gel purified, denatured, mixed, annealed at their *loxP* sites, and reamplified with the outer primers to generate a 3-kb segment with a central *loxP* site at position 66601. This was cut with SphI and SalI and ligated into the same sites of pSP73 (Promega) to make pSP73-loxP1.50. For the second *loxP* site, we PCR amplified genomic coordinates 68080 to 69380, including a *loxP* site (again with spacer region GGATA CTT) at 69380. A second PCR amplified the region of 69380 to 71000, incorporating a *loxP* site at position 69380 and SphI-XbaI sites at position 71000. Again, the two PCR products were gel purified, denatured, mixed, annealed at their *loxP* sites, and reamplified with the outer primers to give a 3-kb product with a central *loxP* site. This was cut with BstBI-XbaI and ligated into psp73-loxP1, cut with the same enzymes (BstBI site at the 3′ end of 50.loxP1 and the XbaI site in psp73) to make pSP73-loxP1.50.loxP2. The mutagenesis construct (consisting of the coordinates 65100 to 66601-*loxP*-66602 to 68084-silent mutation-68085 to 69381-*loxP*-69382 to 71000) was excised with SphI, subcloned into the SphI site of pST76K-SR, and recombined into the MuHV-4 BAC (38) to leave ORF49 (coordinates 66739 to 67644) and ORF50 (66760 to 66795/67661 to 69376) flanked by *loxP* sites at positions 66601 and 69381 (MHV-F50). Viral genome integrity was checked by restriction enzyme digestion, and correct *loxP* site insertion was checked by DNA sequencing across the insertion sites. In a further round of BAC mutagenesis, we combined the F50 mutation with the MHV-GFP cassette (39) to make MHV-F50-GFP. BAC DNA was reconstituted into infectious virus by transfection into BHK-21 cells (Fugene-6; Roche Diagnostics). The floxed BAC/GFP cassette was removed by single passage through NIH 3T3-Cre cells (3 PFU/cell), followed by plaque purification of replication-competent, GFP-negative (GFP$^-$) virus. Stocks were prepared in BHK-21 cells. Infected cell debris was removed by centrifugation (400 × *g*, 5 min), and virions were then recovered from supernatants by ultracentrifugation (38,000 × *g*, 90 min).

Virus assays. To determine titers of infectious MuHV-4, culture-grown stocks or freeze-thawed organ homogenates were plated on BHK-21 monolayers (74). To determine the titer of total reactivatable MuHV-4, organs were disrupted into single-cell suspensions and then plated on BHK-21 cells. The cells were cultured in complete medium for 3 h, overlaid with complete medium plus 0.3% carboxy-methyl-cellulose, cultured for 4 days, fixed with 1% formaldehyde, and stained with 0.1% toluidine blue for plaque counting.

Immunofluorescence. Cells were seeded onto glass coverslips and left to adhere (18 h at 37°C in complete medium). For infection, MuHV-4 was added at the time of seeding (0.3 PFU/cell). The cells were then fixed in phosphate-buffered saline (PBS)–2% formaldehyde (30 min, 23°C), washed, and blocked in PBS–2% bovine serum albumin (BSA)–0.1% Triton X-100 (30 min, 23°C). Viral antigens were detected with

an MuHV-4-specific rabbit serum, raised by two subcutaneous inoculations of MuHV-4 virions (10^9 PFU). The serum recognizes by Western blotting multiple virion proteins, including the products of ORFs 4, 65, and M7 (75). The cells were washed three times in PBS–0.1% Tween 20. Antibody binding was detected with Alexa 555-conjugated donkey anti-rabbit IgG polyclonal antibody (pAb) (Life Technologies). GFP fluorescence was visualized directly. Nuclei were stained with 4′,6′-diamidino-2-phenylindole (DAPI; 1 μg/ml). After a further three washes, the cells were mounted in ProLong Gold (Invitrogen). Images were acquired on a Nikon epifluorescence microscope and analyzed with ImageJ.

Immunostaining. Organs were fixed in 1% formaldehyde–10 mM sodium periodate–75 mM L-lysine (18 h, 4°C), equilibrated in 30% sucrose (24 h, 4°C), and then frozen in 22-oxacalcitriol (OCT). Sections (6 μm) were air dried (1 h, 23°C), washed three times in PBS, blocked with 0.3% Triton X-100–5% normal donkey serum (1 h, 23°C), and incubated (18 h, 4°C) with combinations of antibodies to GFP (rabbit, chicken, or goat pAb), CD11c (hamster monoclonal antibody [MAb] HL-3; BD Pharmingen), surfactant C precursor (goat pAb) (Santa Cruz Biotechnology), olfactory marker protein (goat pAb; Wako Chemicals), CD68 (rat MAb) (FA-11; AbCam), B220 (rat MAb RA3-6B2), CD169 (rat MAb 3D6.112) (Serotec), podoplanin (goat pAb; R&D Systems), and MuHV-4 (rabbit pAb). tdTomato fluorescence was visualized directly. After samples were incubated with the primary antibodies, sections were washed three times in PBS, incubated (1 h, 23°C) with combinations of Alexa 568-donkey anti-rat IgG pAb, Alexa 488- or Alexa 647-donkey anti-rabbit IgG pAb, Alexa 647-donkey anti-mouse IgM pAb, Alexa 488-donkey anti-chicken IgG pAb (Abcam), and Alexa 488-donkey anti-goat pAb (Life Technologies); sections were then washed three times in PBS, nuclei were stained with DAPI, and sections were mounted in Prolong Gold (Life Technologies). tdTomato fluorescence was visualized directly. Images were captured with a Zeiss LCM510 confocal microscope or a Nikon epifluorescence microscope and analyzed with Zen imaging software or ImageJ.

Viral genome quantitation. MuHV-4 genomic coordinates 24832 to 25071 were amplified by PCR (Rotor Gene 3000; Corbett Research) from 10 ng of DNA (NucleoSpin tissue kit; Macherey-Nagel). PCR products quantified with Sybr green (Invitrogen) were compared to a standard curve of cloned template amplified in parallel and distinguished from paired primers by melting curve analysis. Correct sizing was confirmed by electrophoresis and ethidium bromide staining. Cellular DNA in the same samples was quantified by amplifying a β-actin gene fragment.

Flow cytometric sorting. Cells infected with GFP^+ viruses were trypsinized, washed in PBS, and analyzed directly for green channel fluorescence on a BD Accuri 6 cytometer. For sorting, spleens were disrupted into single-cell suspensions. Red cells and dead cells were removed by centrifugation on Ficoll. The cells were washed in PBS–0.1% BSA, incubated (1 h, 4°C) with phycoerythrin-coupled anti-CD19 (BD-Pharmingen), washed two times, and filtered (100-μm pore size). $CD19^+$ cells were collected on a BD FACSAria II and confirmed to be >95% pure on reanalysis. DNA was extracted from the sorted cells for viral genome quantitation.

***In situ* hybridization.** Cells expressing viral tRNAs 1 to 4 were detected by *in situ* hybridization of formalin-fixed, paraffin-embedded spleen cell sections using a digoxigenin-labeled riboprobe (48). Hybridized probe was detected with alkaline phosphatase-conjugated antidigoxigenin Fab fragments (Boehringer Ingelheim).

ACKNOWLEDGMENTS

The work was supported by grants from the Australian Research Council (FT130100138), National Health and Medical Research Council (project grants 1064015, 1079180, and 1122070), Portuguese Fundação para a Ciência e Tecnologia (PTDC/IMI-MIC/0980/2014), and Research Councils UK (BB/J014419/1).

REFERENCES

1. Sunil-Chandra NP, Efstathiou S, Nash AA. 1992. Murine gammaherpesvirus 68 establishes a latent infection in mouse B lymphocytes in vivo. J Gen Virol 73:3275–3279. https://doi.org/10.1099/0022-1317-73-12-3275.
2. Efstathiou S, Ho YM, Minson AC. 1990. Cloning and molecular characterization of the murine herpesvirus 68 genome. J Gen Virol 71:1355–1364. https://doi.org/10.1099/0022-1317-71-6-1355.
3. Virgin HW, Latreille P, Wamsley P, Hallsworth K, Weck KE, Dal Canto AJ, Speck SH. 1997. Complete sequence and genomic analysis of murine gammaherpesvirus 68. J Virol 71:5894–5904.
4. Souza TA, Stollar BD, Sullivan JL, Luzuriaga K, Thorley-Lawson DA. 2005. Peripheral B cells latently infected with Epstein-Barr virus display molecular hallmarks of classical antigen-selected memory B cells. Proc Natl Acad Sci U S A 102:18093–18098. https://doi.org/10.1073/pnas.0509311102.
5. Tarlinton DM. 2008. Evolution in miniature: selection, survival and distribution of antigen reactive cells in the germinal centre. Immunol Cell Biol 86:133–138. https://doi.org/10.1038/sj.icb.7100148.
6. Flaño E, Kim IJ, Woodland DL, Blackman MA. 2002. Gamma-herpesvirus latency is preferentially maintained in splenic germinal center and memory B cells. J Exp Med 196:1363–1372. https://doi.org/10.1084/jem.20020890.
7. Marques S, Efstathiou S, Smith KG, Haury M, Simas JP. 2003. Selective gene expression of latent murine gammaherpesvirus 68 in B lymphocytes. J Virol 77:7308–7318. https://doi.org/10.1128/JVI.77.13.7308-7318.2003.
8. Collins CM, Speck SH. 2012. Tracking murine gammaherpesvirus 68 infection of germinal center B cells in vivo. PLoS One 7:e33230. https://doi.org/10.1371/journal.pone.0033230.
9. Babcock GJ, Decker LL, Volk M, Thorley-Lawson DA. 1998. EBV persistence in memory B cells in vivo. Immunity 9:395–404. https://doi.org/10.1016/S1074-7613(00)80622-6.
10. Willer DO, Speck SH. 2003. Long-term latent murine gammaherpesvirus 68 infection is preferentially found within the surface immunoglobulin D-negative subset of splenic B cells in vivo. J Virol 77:8310–8321. https://doi.org/10.1128/JVI.77.15.8310-8321.2003.
11. Usherwood EJ, Ross AJ, Allen DJ, Nash AA. 1996. Murine gammaherpesvirus-induced splenomegaly: a critical role for CD4 T cells. J Gen Virol 77:627–630. https://doi.org/10.1099/0022-1317-77-4-627.
12. Kim IJ, Flaño E, Woodland DL, Lund FE, Randall TD, Blackman MA. 2003.

Maintenance of long term gamma-herpesvirus B cell latency is dependent on CD40-mediated development of memory B cells. J Immunol 171:886–892. https://doi.org/10.4049/jimmunol.171.2.886.
13. Frederico B, May JS, Efstathiou S, Stevenson PG. 2014. BAFF receptor deficiency limits gammaherpesvirus infection. J Virol 88:3965–3975. https://doi.org/10.1128/JVI.03497-13.
14. Sangster MY, Topham DJ, D'Costa S, Cardin RD, Marion TN, Myers LK, Doherty PC. 2000. Analysis of the virus-specific and nonspecific B cell response to a persistent B-lymphotropic gammaherpesvirus. J Immunol 164:1820–1828. https://doi.org/10.4049/jimmunol.164.4.1820.
15. Thorley-Lawson DA, Miyashita EM, Khan G. 1996. Epstein-Barr virus and the B cell: that's all it takes. Trends Microbiol 4:204–208. https://doi.org/10.1016/S0966-842X(96)90020-7.
16. Hoagland RJ. 1955. The transmission of infectious mononucleosis. Am J Med Sci 229:262–272. https://doi.org/10.1097/00000441-195503000-00003.
17. Hoagland RJ. 1964. The incubation period of infectious mononucleosis. Am J Public Health Nations Health 54:1699–1705. https://doi.org/10.2105/AJPH.54.10.1699.
18. Dunmire SK, Grimm JM, Schmeling DO, Balfour HH, Jr, Hogquist KA. 2015. The incubation period of primary Epstein-Barr virus infection: viral dynamics and immunologic events. PLoS Pathog 11:e1005286. https://doi.org/10.1371/journal.ppat.1005286.
19. Janz A, Oezel M, Kurzeder C, Mautner J, Pich D, Kost M, Hammerschmidt W, Delecluse HJ. 2000. Infectious Epstein-Barr virus lacking major glycoprotein BLLF1 (gp350/220) demonstrates the existence of additional viral ligands. J Virol 74:10142–10152. https://doi.org/10.1128/JVI.74.21.10142-10152.2000.
20. Hutt-Fletcher LM. 2007. Epstein-Barr virus entry. J Virol 81:7825–7832. https://doi.org/10.1128/JVI.00445-07.
21. Frederico B, Milho R, May JS, Gillet L, Stevenson PG. 2012. Myeloid infection links epithelial and B cell tropisms of murid herpesvirus-4. PLoS Pathog 8:e1002935. https://doi.org/10.1371/journal.ppat.1002935.
22. Balfour HH. 2014. Progress, prospects, and problems in Epstein-Barr virus vaccine development. Curr Opin Virol 6:1–5. https://doi.org/10.1016/j.coviro.2014.02.005.
23. Milho R, Smith CM, Marques S, Alenquer M, May JS, May JS, Gillet L, Gaspar M, Efstathiou S, Simas JP, Stevenson PG. 2009. In vivo imaging of murid herpesvirus-4 infection. J Gen Virol 90:21–32. https://doi.org/10.1099/vir.0.006569-0.
24. Milho R, Frederico B, Efstathiou S, Stevenson PG. 2012. A heparan-dependent herpesvirus targets the olfactory neuroepithelium for host entry. PLoS Pathog 8:e1002986. https://doi.org/10.1371/journal.ppat.1002986.
25. Shivkumar M, Milho R, May JS, Nicoll MP, Efstathiou S, Stevenson PG. 2013. Herpes simplex virus 1 targets the murine olfactory neuroepithelium for host entry. J Virol 87:10477–10488. https://doi.org/10.1128/JVI.01748-13.
26. Farrell HE, Lawler C, Tan CS, MacDonald K, Bruce K, Mach M, Davis-Poynter N, Stevenson PG. 2016. Murine cytomegalovirus exploits olfaction to enter new hosts. mBio 7:e00251-16. https://doi.org/10.1128/mBio.00251-16.
27. Gaspar M, May JS, Sukla S, Frederico B, Gill MB, Smith CM, Belz GT, Stevenson PG. 2011. Murid herpesvirus-4 exploits dendritic cells to infect B cells. PLoS Pathog 7:e1002346. https://doi.org/10.1371/journal.ppat.1002346.
28. Usherwood EJ, Stewart JP, Robertson K, Allen DJ, Nash AA. 1996. Absence of splenic latency in murine gammaherpesvirus 68-infected B cell-deficient mice. J Gen Virol 77:2819–2825. https://doi.org/10.1099/0022-1317-77-11-2819.
29. Chao B, Frederico B, Stevenson PG. 2015. B-cell-independent lymphoid tissue infection by a B-cell-tropic rhadinovirus. J Gen Virol 96:2788–2793. https://doi.org/10.1099/vir.0.000188.
30. Frederico B, Chao B, May JS, Belz GT, Stevenson PG. 2014. A murid gamma-herpesviruses exploits normal splenic immune communication routes for systemic spread. Cell Host Microbe 15:457–470. https://doi.org/10.1016/j.chom.2014.03.010.
31. Simas JP, Efstathiou S. 1998. Murine gammaherpesvirus 68: a model for the study of gammaherpesvirus pathogenesis. Trends Microbiol 6:276–282. https://doi.org/10.1016/S0966-842X(98)01306-7.
32. McHeyzer-Williams M, Okitsu S, Wang N, McHeyzer-Williams L. 2011. Molecular programming of B cell memory. Nat Rev Immunol 12:24–34. https://doi.org/10.1038/nri3128.
33. Zabel F, Mohanan D, Bessa J, Link A, Fettelschoss A, Saudan P, Kündig TM, Bachmann MF. 2014. Viral particles drive rapid differentiation of memory B cells into secondary plasma cells producing increased levels of antibodies. J Immunol 192:5499–5508. https://doi.org/10.4049/jimmunol.1400065.
34. Seifert M, Przekopowitz M, Taudien S, Lollies A, Ronge V, Drees B, Lindemann M, Hillen U, Engler H, Singer BB, Küppers R. 2015. Functional capacities of human IgM memory B cells in early inflammatory responses and secondary germinal center reactions. Proc Natl Acad Sci U S A 112:E546–E555. https://doi.org/10.1073/pnas.1416276112.
35. Wu TT, Tong L, Rickabaugh T, Speck S, Sun R. 2001. Function of Rta is essential for lytic replication of murine gammaherpesvirus 68. J Virol 75:9262–9273. https://doi.org/10.1128/JVI.75.19.9262-9273.2001.
36. Moser JM, Farrell ML, Krug LT, Upton JW, Speck SH. 2006. A gammaherpesvirus 68 gene 50 null mutant establishes long-term latency in the lung but fails to vaccinate against a wild-type virus challenge. J Virol 80:1592–1598. https://doi.org/10.1128/JVI.80.3.1592-1598.2006.
37. Noh CW, Cho HJ, Kang HR, Jin HY, Lee S, Deng H, Wu TT, Arumugaswami V, Sun R, Song MJ. 2012. The virion-associated open reading frame 49 of murine gammaherpesvirus 68 promotes viral replication both in vitro and in vivo as a derepressor of RTA. J Virol 86:1109–1118. https://doi.org/10.1128/JVI.05785-11.
38. Adler H, Messerle M, Wagner M, Koszinowski UH. 2000. Cloning and mutagenesis of the murine gammaherpesvirus 68 genome as an infectious bacterial artificial chromosome. J Virol 74:6964–6974. https://doi.org/10.1128/JVI.74.15.6964-6974.2000.
39. May JS, Stevenson PG. 2010. Vaccination with murid herpesvirus-4 glycoprotein B reduces viral lytic replication but does not induce detectable virion neutralization. J Gen Virol 91:2542–2552. https://doi.org/10.1099/vir.0.023085-0.
40. May JS, Bennett NJ, Stevenson PG. 2010. An in vitro system for studying murid herpesvirus-4 latency and reactivation. PLoS One 5:e11080. https://doi.org/10.1371/journal.pone.0011080.
41. Schwenk F, Sauer B, Kukoc N, Hoess R, Müller W, Kocks C, Kühn R, Rajewsky K. 1997. Generation of Cre recombinase-specific monoclonal antibodies, able to characterize the pattern of Cre expression in cre-transgenic mouse strains. J Immunol Methods 207:203–212. https://doi.org/10.1016/S0022-1759(97)00116-6.
42. Rickert RC, Roes J, Rajewsky K. 1997. B lymphocyte-specific, Cre-mediated mutagenesis in mice. Nucleic Acids Res 25:1317–1318. https://doi.org/10.1093/nar/25.6.1317.
43. Liang X, Collins CM, Mendel JB, Iwakoshi NN, Speck SH. 2009. Gammaherpesvirus-driven plasma cell differentiation regulates virus reactivation from latently infected B lymphocytes. PLoS Pathog 5:e1000677. https://doi.org/10.1371/journal.ppat.1000677.
44. Stashenko P, Nadler LM, Hardy R, Schlossman SF. 1981. Expression of cell surface markers after human B lymphocyte activation. Proc Natl Acad Sci U S A 78:3848–3852.
45. Smith CM, Gill MB, May JS, Stevenson PG. 2007. Murine gammaherpesvirus-68 inhibits antigen presentation by dendritic cells. PLoS One 2:e1048. https://doi.org/10.1371/journal.pone.0001048.
46. Dyson PJ, Farrell PJ. 1985. Chromatin structure of Epstein-Barr virus. J Gen Virol 66:1931–1940. https://doi.org/10.1099/0022-1317-66-9-1931.
47. Long MA, Rossi FM. 2009. Silencing inhibits Cre-mediated recombination of the Z/AP and Z/EG reporters in adult cells. PLoS One 4:e5435. https://doi.org/10.1371/journal.pone.0005435.
48. Bowden RJ, Simas JP, Davis AJ, Efstathiou S. 1997. Murine gammaherpesvirus 68 encodes tRNA-like sequences which are expressed during latency. J Gen Virol 78:1675–1687. https://doi.org/10.1099/0022-1317-78-7-1675.
49. Coleman HM, Efstathiou S, Stevenson PG. 2005. Transcription of the murine gammaherpesvirus 68 ORF73 from promoters in the viral terminal repeats. J Gen Virol 86:561–574. https://doi.org/10.1099/vir.0.80565-0.
50. Stevenson PG, Belz GT, Altman JD, Doherty PC. 1999. Changing patterns of dominance in the CD8$^+$ T cell response during acute and persistent murine gamma-herpesvirus infection. Eur J Immunol 29:1059–1067. https://doi.org/10.1002/(SICI)1521-4141(199904)29:04<1059::AID-IMMU1059>3.0.CO;2-L.
51. Callan MF, Steven N, Krausa P, Wilson JD, Moss PA, Gillespie GM, Bell JI, Rickinson AB, McMichael AJ. 1996. Large clonal expansions of CD8$^+$ T cells in acute infectious mononucleosis. Nat Med 2:906–911. https://doi.org/10.1038/nm0896-906.
52. Siegel AM, Rangaswamy US, Napier RJ, Speck SH. 2010. Blimp-1-dependent plasma cell differentiation is required for efficient mainte-

nance of murine gammaherpesvirus latency and antiviral antibody responses. J Virol 84:674–685. https://doi.org/10.1128/JVI.01306-09.
53. Herskowitz JH, Jacoby MA, Speck SH. 2005. The murine gammaherpesvirus 68 M2 gene is required for efficient reactivation from latently infected B cells. J Virol 79:2261–2273. https://doi.org/10.1128/JVI.79.4.2261-2273.2005.
54. Simas JP, Marques S, Bridgeman A, Efstathiou S, Adler H. 2004. The M2 gene product of murine gammaherpesvirus 68 is required for efficient colonization of splenic follicles but is not necessary for expansion of latently infected germinal centre B cells. J Gen Virol 85:2789–2797. https://doi.org/10.1099/vir.0.80138-0.
55. Elliott SL, Suhrbier A, Miles JJ, Lawrence G, Pye SJ, Le TT, Rosenstengel A, Nguyen T, Allworth A, Burrows SR, Cox J, Pye D, Moss DJ, Bharadwaj M. 2008. Phase I trial of a CD8$^+$ T-cell peptide epitope-based vaccine for infectious mononucleosis. J Virol 82:1448–1457. https://doi.org/10.1128/JVI.01409-07.
56. Mautner J, Bornkamm GW. 2012. The role of virus-specific CD4$^+$ T cells in the control of Epstein-Barr virus infection. Eur J Cell Biol 91:31–35. https://doi.org/10.1016/j.ejcb.2011.01.007.
57. Marques S, Alenquer M, Stevenson PG, Simas JP. 2008. A single CD8$^+$ T cell epitope sets the long-term latent load of a murid herpesvirus. PLoS Pathog 4:e1000177. https://doi.org/10.1371/journal.ppat.1000177.
58. Usherwood EJ, Ward KA, Blackman MA, Stewart JP, Woodland DL. 2001. Latent antigen vaccination in a model gammaherpesvirus infection. J Virol 75:8283–8288. https://doi.org/10.1128/JVI.75.17.8283-8288.2001.
59. Boname JM, Coleman HM, May JS, Stevenson PG. 2004. Protection against wild-type murine gammaherpesvirus-68 latency by a latency-deficient mutant. J Gen Virol 85:131–135. https://doi.org/10.1099/vir.0.19592-0.
60. Fowler P, Efstathiou S. 2004. Vaccine potential of a murine gammaherpesvirus-68 mutant deficient for ORF73. J Gen Virol 85:609–613. https://doi.org/10.1099/vir.0.19760-0.
61. Jia Q, Freeman ML, Yager EJ, McHardy I, Tong L, Martinez-Guzman D, Rickabaugh T, Hwang S, Blackman MA, Sun R, Wu TT. 2010. Induction of protective immunity against murine gammaherpesvirus 68 infection in the absence of viral latency. J Virol 84:2453–2465. https://doi.org/10.1128/JVI.01543-09.
62. Tan CSE, Lawler C, Stevenson PG. 2017. CD8$^+$ T cell evasion mandates CD4$^+$ T cell control of chronic gamma-herpesvirus infection. PLoS Pathog 13:e1006311. https://doi.org/10.1371/journal.ppat.1006311.
63. Stevenson PG, Belz GT, Castrucci MR, Altman JD, Doherty PC. 1999. A gamma-herpesvirus sneaks through a CD8$^+$ T cell response primed to a lytic-phase epitope. Proc Natl Acad Sci U S A 96:9281–9286. https://doi.org/10.1073/pnas.96.16.9281.
64. Martin DF, Kuppermann BD, Wolitz RA, Palestine AG, Li H, Robinson CA. 1999. Oral ganciclovir for patients with cytomegalovirus retinitis treated with a ganciclovir implant. Roche Ganciclovir Study Group. N Engl J Med 340:1063–1070. https://doi.org/10.1056/NEJM199904083401402.
65. Yao QY, Ogan P, Rowe M, Wood M, Rickinson AB. 1989. The Epstein-Barr virus:host balance in acute infectious mononucleosis patients receiving acyclovir anti-viral therapy. Int J Cancer 43:61–66. https://doi.org/10.1002/ijc.2910430114.
66. Hoshino Y, Katano H, Zou P, Hohman P, Marques A, Tyring SK, Follmann D, Cohen JI. 2009. Long-term administration of valacyclovir reduces the number of Epstein-Barr virus (EBV)-infected B cells but not the number of EBV DNA copies per B cell in healthy volunteers. J Virol 83:11857–11861. https://doi.org/10.1128/JVI.01005-09.
67. Meerbach A, Holý A, Wutzler P, De Clercq E, Neyts J. 1998. Inhibitory effects of novel nucleoside and nucleotide analogues on Epstein-Barr virus replication. Antivir Chem Chemother 9:275–282. https://doi.org/10.1177/095632029800900309.
68. Caton ML, Smith-Raska MR, Reizis B. 2007. Notch-RBP-J signaling controls the homeostasis of CD8$^-$ dendritic cells in the spleen. J Exp Med 204:1653–1664. https://doi.org/10.1084/jem.20062648.
69. Clausen BE, Burkhardt C, Reith W, Renkawitz R, Förster I. 1999. Conditional gene targeting in macrophages and granulocytes using LysMcre mice. Transgenic Res 8:265–277. https://doi.org/10.1023/A:1008942828960.
70. Tan CS, Frederico B, Stevenson PG. 2014. Herpesvirus delivery to the murine respiratory tract. J Virol Methods 206:105–114. https://doi.org/10.1016/j.jviromet.2014.06.003.
71. Stevenson PG, May JS, Smith XG, Marques S, Adler H, Koszinowski UH, Simas JP, Efstathiou S. 2002. K3-mediated evasion of CD8$^+$ T cells aids amplification of a latent gamma-herpesvirus. Nat Immunol 3:733–740.
72. Song MJ, Hwang S, Wong WH, Wu TT, Lee S, Liao HI, Sun R. 2005. Identification of viral genes essential for replication of murine gamma-herpesvirus 68 using signature-tagged mutagenesis. Proc Natl Acad Sci U S A 102:3805–3810. https://doi.org/10.1073/pnas.0404521102.
73. Liu S, Pavlova IV, Virgin HW, Speck SH. 2000. Characterization of gammaherpesvirus 68 gene 50 transcription. J Virol 74:2029–2037. https://doi.org/10.1128/JVI.74.4.2029-2037.2000.
74. de Lima BD, May JS, Stevenson PG. 2004. Murine gammaherpesvirus 68 lacking gp150 shows defective virion release but establishes normal latency in vivo. J Virol 78:5103–5112. https://doi.org/10.1128/JVI.78.10.5103-5112.2004.
75. Gillet L, Adler H, Stevenson PG. 2007. Glycosaminoglycan interactions in murine gammaherpesvirus-68 infection. PLoS One 2:e347. https://doi.org/10.1371/journal.pone.0000347.